Design of an adaptive sliding mode controller for robust yaw stabilisation of in-wheel-motor-driven electric vehicles

Kanghyun Nam*

Samsung Electronics Co., Ltd.,
Suwon, Gyeonggi-do, South Korea
Email: nkh6189@gmail.com
*Corresponding author

Hiroshi Fujimoto and Yoichi Hori

Department of Advanced Energy,
The University of Tokyo,
Kashiwa, Chiba 277-8561, Japan
Email: fujimoto@k.u-tokyo.ac.jp
Email: hori@k.u-tokyo.ac.jp

Abstract: A robust yaw stability control system is designed to stabilise the vehicle yaw motion. Vehicles undergo changes in parameters and disturbances with respect to the wide range of driving conditions, e.g., tyre-road conditions. Therefore, a robust control design technique is required to guarantee system stability and enhance the robustness. In this paper, a sliding mode control methodology is applied to make vehicle yaw rate to track its reference with robustness against model uncertainties and disturbances. In addition, a parameter adaptation law is also applied to estimate varying vehicle parameters with respect to road conditions and is incorporated into sliding mode control framework. The control performance of the proposed control system was evaluated through field tests.

Keywords: adaptive sliding mode control; in-wheel motor-driven electric vehicle; yaw stabilisation.

Reference to this paper should be made as follows: Nam, K., Fujimoto, H. and Hori, Y. (2015) 'Design of an adaptive sliding mode controller for robust yaw stabilisation of in-wheel-motor-driven electric vehicles', *Int. J. Vehicle Design*, Vol. 67, No. 1, pp.98–113.

Biographical notes: Kanghyun Nam received the BS in Mechanical Engineering from Kyungpook National University, Daegu, Korea, in 2007, the MS in Mechanical Engineering from Korea Advanced Institute of Science and Technology, Daejeon, Korea, in 2009, and the PhD in Electrical Engineering from The University of Tokyo, Tokyo, Japan, 2012. He is now working for Samsung Electronics Co., Ltd., Gyeonggi-do, Korea, as a Senior Engineer. His research interests include vehicle dynamics and control, state estimation and motion control for electric vehicles, mechatronic, and precision motion control.

Hiroshi Fujimoto received the PhD in the Department of Electrical Engineering from the University of Tokyo in 2001. In 2001, he joined the Department of Electrical Engineering, Nagaoka University of Technology, Niigata, Japan, as a research associate. From 2002 to 2003, he was a visiting scholar in the School of Mechanical Engineering, Purdue University, USA. In 2004, he joined the Department of Electrical and Computer Engineering, Yokohama National University, Yokohama, Japan, as a lecturer and he became an Associate Professor in 2005. He is currently an associate professor of the University of Tokyo since 2010. He received the Best Paper Award from the IEEE Transaction On Industrial Electronics in 2001, Isao Takahashi Power Electronics Award in 2010, and Best Author Prize of SICE in 2010. His interests are in control engineering, motion control, nano-scale servo systems, electric vehicle control, and motor drive.

Yoichi Hori received his BS, MS, and PhD in Electrical Engineering from the University of Tokyo, Tokyo, Japan, in 1978, 1980, and 1983, respectively. In 1983, he joined the Department of Electrical Engineering, The University of Tokyo, as a Research Associate. He later became an Assistant Professor, an Associate Professor, and, in 2000, a Professor at the same university. In 2002, he moved to the Institute of Industrial Science as a Professor in the Information and System Division, and in 2008, to the Department of Advanced Energy, Graduate School of Frontier Sciences, the University of Tokyo. From 1991 to 1992, he was a Visiting Researcher at the University of California at Berkeley. His research fields are control theory and its industrial applications to motion control, mechatronics, robotics, electric vehicles.

This paper is a revised and expanded version of a paper entitled 'Design of adaptive sliding mode controller for robust yaw stabilisation of in-wheel-motor-driven electric vehicles' presented at *EVS26*, Los Angeles, California, 6–9 May, 2012.

1 Introduction

Owing to the increasing concerns about advanced motion control of electric vehicles with in-wheel motors, a great deal of research on dynamics control for electric vehicles has been carried out since 2000 (Hori, 2004; Magallan et al., 2011; Yin et al., 2009; Wang et al., 2011; Mutoh et al., 2012; Nam et al., 2012a). Advanced motion control systems for electric vehicles, slip prevention, spinout prevention, and excessive roll prevention, are referred to as yaw stability control and roll stability control, respectively. Compared with internal combustion engine vehicles, electric vehicles with in-wheel motors have several advantages from the viewpoint of motion control (Hori, 2004; Yin et al., 2009).

- the torque generation of driving motors is very fast and accurate
- the driving torque can be easily measured from motor current
- each wheel with an in-wheel motor can be independently controlled.

The purpose of vehicle motion controls is to prevent unintended vehicle behaviour through active vehicle control and assist drivers in maintaining controllability and stability of vehicles. The main goal of most motion control systems is to control the yaw rate of the vehicles. In Cong et.al. (2009), direct yaw moment control based on side slip angle

estimation was proposed for improving the stability of in-wheel-motor-driven electric vehicles (IWM-EV). A fuzzy-rule-based control and sliding mode control algorithms for vehicle stability enhancement were proposed and evaluated through experiments (Kim et al., 2008, 2010; Tchamna et al., 2013). A novel yaw stability control method based on robust yaw moment observer (YMO) design was presented and its practical effectiveness was verified through various field tests (Fujimoto et al., 2005). Parameter uncertainties shown in a vehicle model and external disturbances acting on vehicles are compensated by the disturbance observer and yaw stabilisation is realised through yaw rate feedback control. In this paper, a sliding model control method with parameter adaptation is employed for robust yaw stabilisation of electric vehicles. The proposed control structure employs a reference generator, which is designed from driver's commands, a sliding mode controller, and parameter adaptation laws. The sliding mode control technique is well-known robust control methodology particularly suitable for dealing with nonlinear systems with model uncertainties and disturbances like the considered vehicle systems. Since the vehicles operate under a wide range of road conditions and speeds, the controller should provide robustness against varying parameters and undesired disturbances all over the driving regions. In Zhou et al. (2010), a cascade vehicle yaw stability control system was designed with the sliding mode and backstepping control approaches. In Canale et al. (2008), a vehicle yaw controller via second-order sliding mode technique was designed to guarantee robust stability in front of disturbances and model uncertainties.

In order to compensate for the disturbances and model uncertainties existing in control law, the adaptive sliding mode control method is applied. By combining with the defined sliding surface, a sliding mode controller is re-designed such that the state (i.e., yaw rate) is moved from the outside to inside of the region, and finally, it remains inside the region even though there are model uncertainties and disturbances, which can be estimated and then rejected by adaptation law.

In order to verify the control performances, experiments are performed using an IWM-EV which was developed by the Hori/Fujimoto research team (see Nam et al., 2011, 2012b), and compared with test data.

This paper is organised as follows. A vehicle model for control design is introduced in Section 2. A sliding mode controller combining parameter adaptation approaches is proposed and the stability of both a sliding mode control law and an adaptation law is proved in Section 3. The experiment results are presented and discussed in Section 4. Finally, conclusions and future works are presented.

2 Vehicle model

In this section, a yaw plane model is introduced to describe the motion of an in-wheel-motor driven electric vehicle. The main difference from commonly used vehicle dynamics is that the direct yaw moment can be an additional input variable, which is generated by motor torque difference between each wheel. The yaw plane representation with direct yaw moment is shown in Figure 1.

From the linear single track vehicle model as shown in Figure 1(b), the governing equation for yaw motion is given by

$$I_z\dot{\gamma} = l_f F_f^y \cos\delta_f - l_r F_r^y + M_z \tag{1}$$

where γ is the yaw rate, I_z is the yaw moment of inertia, F_f^y and F_r^y are the front and rear lateral tyre forces, respectively, l_f and l_r are the distance from vehicle centre of gravity (CG) to front and rear axles, δ_f is the front steering angle, and the yaw moment M_z indicates a direct yaw moment control input, which is generated by the independent torque control of in-wheel motors and is used to stabilise the vehicle motion, and can be calculated as follows:

$$M_z = \frac{d}{2}(F_{rr}^x - F_{rl}^x) + \frac{d}{2}(F_{fr}^x - F_{fl}^x)\cos\delta_f. \tag{2}$$

Here, longitudinal tyre forces, $F_{fl}^x, F_{fr}^x, F_{rl}^x$, and F_{rr}^x, are generated by driving motors' torques and can be obtained from a driving force observer (shown in Figure 2), which is designed based on wheel rotational motion, and the estimate of longitudinal tyre forces is expressed as

$$\hat{F}_i^x = \frac{\omega_D}{s+\omega_D}\left(\frac{T_i^m - I_\omega \omega_i s}{r}\right) \tag{3}$$

where $\hat{F}_i^x$ is the estimated longitudinal tyre force at ith wheel, T_i^m is the motor torque acting on each wheel, I_ω is the wheel inertia, ω_i is an angular velocity of the wheel, r is an effective tyre radius, and ω_D is a cutoff frequency of the applied low-pass filter which rejects high frequency noises caused by time derivative of ω_i.

Figure 1 Planar vehicle model: (a) four wheel model and (b) single track model (i.e., bicycle model)

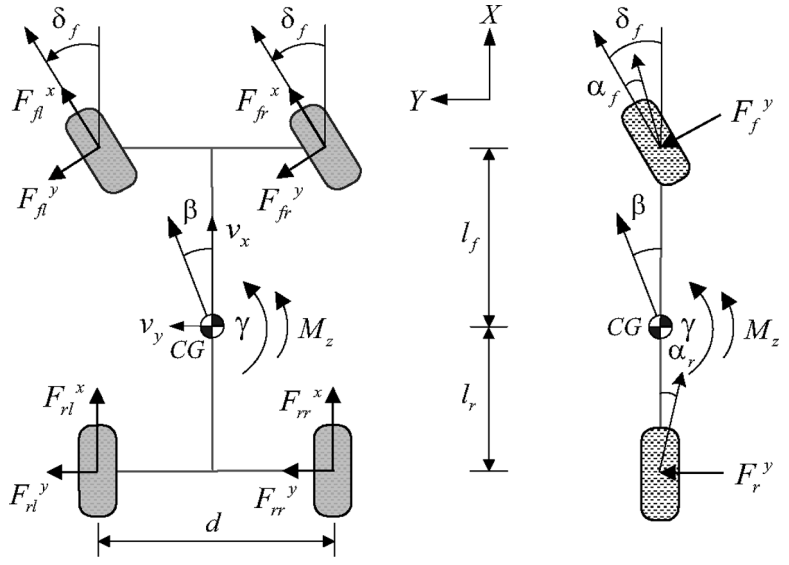

In order to describe the vehicle motion, a linear tyre model is used. For small tyre slip angles, the lateral tyre forces can be linearly approximated as follows:

$$F_f^y = -2C_f\alpha_f = -2C_f\left(\frac{v_y + \gamma l_f}{v_x} - \delta_f\right) = -2C_f\left(\beta + \frac{\gamma l_f}{v_x} - \delta_f\right) \tag{4}$$

$$F_r^y = -2C_r\alpha_r = -2C_r\left(\frac{v_y - \gamma l_r}{v_x}\right) = -2C_r\left(\beta - \frac{\gamma l_r}{v_x}\right) \tag{5}$$

where β is a vehicle sideslip angle, v_x is the longitudinal vehicle velocity, v_y is the lateral vehicle velocity, α_f and α_r are tyre slip angles of front and rear tyres, and C_f and C_r are the front and rear tyre cornering stiffness, respectively.

Figure 2 (a) Wheel rotational motion and (b) block diagram of Driving force observer (DFO) (see online version for colours)

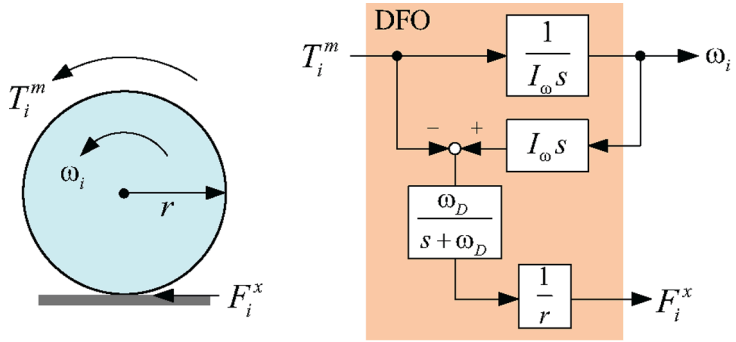

(a) (b)

From equations (1), (4), and (5), the dynamic equation for yaw motion is expressed as

$$I_z\dot{\gamma} = -\frac{2(l_f^2C_f + l_r^2C_r)}{v_x}\gamma + 2l_fC_f\delta_f - 2\beta(l_fC_f - l_rC_r) + M_z + M_d. \tag{6}$$

Here, $\bar{M}_d$ is newly defined as a lumped yaw moment disturbance including external disturbances and unmeasurable moment terms, i.e., $2\beta(l_fC_f - l_rC_r)$,

$$\bar{M}_d = -2\beta(l_fC_f - l_rC_r) + M_d \tag{7}$$

where, since it is difficult to accurately measure or estimate the β, a moment term generated by β is considered as a disturbance. M_d is the yaw moment disturbance mainly caused by lateral wind, unbalanced left/right road conditions, and unbalanced left/right tyre pressure.

Assumption: The lumped disturbance $\bar{M}_d(t)$, which varies with tyre-road condition and vehicle parameters, is bounded and satisfy the following inequality condition.

$$\|\bar{M}_d(t)\| \leq \Upsilon \tag{8}$$

where Υ is the upper bound of the lumped disturbance.

Consequentially, yaw dynamics (equation (6)) is expressed as a following equation that has two inputs and one output,

$$I_z\dot{\gamma} = -\frac{2B}{v_x(t)}\gamma + 2l_fC_f\delta_f + M_z + \bar{M}_d \tag{9}$$

where $B = l_f^2C_f + l_r^2C_r$.

Here B is defined as a yaw damping coefficient which varies with tyre cornering stiffness.

3 Design of an adaptive sliding mode controller

3.1 Overall control structure

The proposed control system is depicted in Figure 3. A reference generator makes a desired yaw rate γ_d from driver's steering command δ_{cmd} and vehicle speed v_x. The feedback controller is designed to make yaw moment to compensate yaw rate tracking error (i.e., $\gamma_d - \gamma$) based on the standard sliding mode control methodology. For treating model uncertainties and disturbances existing in a feedback control law, parameters in a designed sliding mode control law are updated according to adaptation laws. The external input M_d accounts for yaw moment disturbance caused by lateral wind, unbalanced road conditions, and unbalanced tyre pressure,etc. With well-tuned control parameters, a proposed controller contributes to keeping the vehicle yaw rate following its target commanded by the driver.

Figure 3 Block diagram of an adaptive sliding mode controller (see online version for colours)

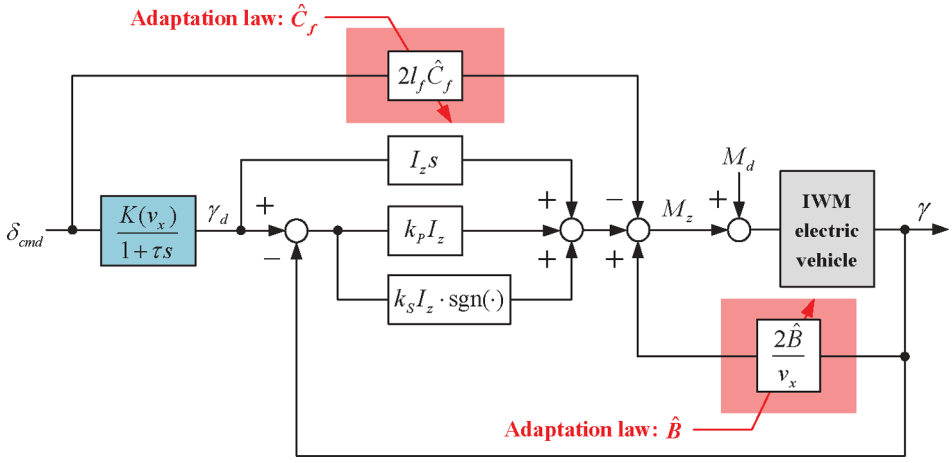

3.2 Reference generation: desired yaw response

The objective of the yaw stability control is to improve the vehicle steadiness and transient response properties, enhancing vehicle handling performance and maintaining stability in those cornering maneuvers, i.e., the yaw rate γ should be close to desired yaw responses (i.e., γ_d). The desired vehicle response is defined based on driver's cornering intention (e.g., driver's steering command and vehicle speed). Desired vehicle yaw rate response for given steering angle and vehicle speed is obtained as follows:

$$\gamma_d = \frac{K(v_x)}{1+\tau s} \cdot \delta_{\text{cmd}}. \tag{10}$$

Here,

$$K(v_x) = \frac{1}{1+k_{us}v_x^2}\frac{v_x}{l}, \quad k_{us} = \frac{m(l_r C_r - l_f C_f)}{2l^2 C_f C_r}$$

where τ is a cutoff frequency of the desired model filter, k_{us} is a vehicle stability factor which explains the steering characteristics of the vehicles. The sign of $l_r C_r - l_f C_f$ in k_{us} represents the vehicle motion behaviour by steering action and the steering characteristics are classified as follows:

$$\begin{aligned} &l_r C_r - l_f C_f > 0 \quad \text{: under steering} \\ &l_r C_r - l_f C_f = 0 \quad \text{: neutral steering} \\ &l_r C_r - l_f C_f < 0 \quad \text{: over steering.} \end{aligned} \tag{11}$$

3.3 Sliding mode control

It is well known that sliding mode control is a robust control method to stabilise nonlinear and uncertain systems which have attractive features to keep the systems insensitive to the uncertainties on the sliding surface (Slotine et al., 1991). The conventional sliding mode control design approach consists of two steps. First, a sliding surface is designed such that the system trajectory along the surface acquires certain desired properties. Then, a discontinuous control is designed such that the system trajectories reach the sliding surface in finite time. A sliding mode control as a general design technique for control systems has been well established, the advantages of a sliding model control method are:

- fast response and good transient performance
- its robustness against a large class of perturbations or model uncertainties
- the possibility of stabilising some complex nonlinear systems which are difficult to stabilise by continuous state feedback laws.

Based on above advantages, sliding mode control has been applied to vehicle control systems Zhou et al. (2010) and Canale et al. (2008). As usual in the sliding mode control technique, the control forces the system evolution on a certain surface which guarantees the achievement of the control requirements. In order to achieve control objective, i.e., $\lim_{t\to\infty} S(t) = 0$, the sliding surface $S(t)$ is defined as

$$S = \gamma - \gamma_d. \tag{12}$$

Here we can see that the sliding condition $S(t) = 0$ means a zero tracking error.

By designing a satisfactory dynamics feedback control law, the trajectory of the closed-loop system can be driven on the sliding surface (equation (12)) and evolve along it, and yaw stabilisation can be achieved. In order to achieve control requirements, a following reaching condition to be satisfied is designed as

$$\dot{S} = -k_P S - k_S \cdot \text{sgn}(S) \tag{13}$$

where it is noted that by adding the proportional rate term $-k_P S$, the state is forced to approach the sliding surface faster when S is large enough (Gao et al., 1993). The $k_P > 0$ is a control parameter which determines the convergence rate of a tracking error, the $k_S > 0$ is a control parameter which should be tunned according to bound of uncertainties and disturbances.

From equations (9), (12), and (13), we can apply a standard sliding mode control method (Slotine et al., 1991) and thereby the following control law can be obtained

$$M_z(t) \;=\; I_z\dot{\gamma}_d(t) + \frac{2B}{v_x(t)}\gamma(t) - 2l_fC_f\delta_f(t) - k_PI_z\mathrm{S} - k_SI_z\cdot\mathrm{sgn(S)}. \tag{14}$$

We can prove that the sliding mode control law (equation (14)) makes the closed-loop control system asymptotically stable by introducing following positive definite Lyapunov function

$$V = \frac{1}{2}S^2. \tag{15}$$

The time derivative of equation (15) is

$$\begin{aligned}\dot{V} = \mathrm{S}\dot{\mathrm{S}} \;&=\; \mathrm{S}(\dot{\gamma}-\dot{\gamma}_d) = \mathrm{S}\left[-\frac{2B}{I_zv_x}\gamma \;+\; \frac{2l_fC_f\delta_f}{I_z} + \frac{M_z}{I_z} + \frac{\bar{M}_d}{I_z} - \dot{\gamma}_d\right]\\ &=\; \mathrm{S}\left[-k_P\mathrm{S} - k_S\cdot\mathrm{sgn(S)} + \frac{\bar{M}_d}{I_z}\right] \;\le -k_P\mathrm{S}^2 - k_S|\mathrm{S}| + |S|\cdot\left|\frac{\bar{M}_d}{I_z}\right|.\end{aligned} \tag{16}$$

Defining $\Gamma = \sup_{t\geq 0}\left|\frac{\bar{M}_d}{I_z}\right|$, we find that if $k_S > \Gamma$,

$$\begin{aligned}\dot{V} \;&\le -k_P\mathrm{S}^2 - k_S|\mathrm{S}| + |S|\cdot\left|\frac{\bar{M}_d}{I_z}\right| \;= -k_P\mathrm{S}^2 - |\mathrm{S}|\cdot\left(k_S - \left|\frac{\bar{M}_d}{I_z}\right|\right)\\ &\le -k_P\mathrm{S}^2 - (k_S-\Gamma)|\mathrm{S}| \;< 0.\end{aligned} \tag{17}$$

Thus, the control objective, i.e., $S(t)\to 0$ as $t\to\infty$, can be achieved by the control law (equation (14)).

Remark 1: In equation (14), the sliding mode switching gain k_S is selected considering uncertainty and disturbance bound. From assumption (equation (8)), k_S should be determined by considering the disturbance bound. Moreover, the maximum k_S which can be selected is limited by the maximum torque that an in-wheel motor generates. By properly tuning k_P and k_S, the chattering in control law is also reduced.

3.4 Sliding mode control with parameter adaptation

For treating the disturbance and parameter uncertainty existing in the control law (equation (14)), adaptive control method is a natural choice and has been widely applied. Combined with the defined sliding surface, a sliding mode controller can be designed such that the system state is moved from the outside to the inside of the region, and finally remains inside the region in spite of the uncertainty and disturbance which can be estimated and then rejected under the help of adaptive law. Thus, based on above analysis, the control law (equation (14)) is modified as

$$M_z(t) \;=\; I_z\dot{\gamma}_d(t) + \frac{2\hat{B}}{v_x(t)}\gamma(t) - 2l_f\hat{C}_f\delta_f(t) - k_PI_z\mathrm{S} - k_SI_z\cdot\mathrm{sgn(S)} \tag{18}$$

where the adaptation law for the estimated parameters $\hat{B}$ and $\hat{C}_f$ is chosen as

$$\dot{\hat{B}}(t) = -\frac{2k_1}{I_z v_x(t)}\gamma(t)\mathrm{S} - \eta_1 k_1 \tilde{B} \tag{19}$$

$$\dot{\hat{C}}_f(t) = -\frac{2l_f k_2}{I_z}\delta_f(t)\mathrm{S} - \eta_2 k_2 \tilde{C}_f. \tag{20}$$

Here $\tilde{B} = \hat{B}(t) - B$, $\tilde{C}_f = \hat{C}_f(t) - C_f$, k_1 and k_2 are adaptation gains which determine the update rate, η_1 and η_2 are positive constant values.

Remark 2: The main objective of parameter adaptation is to compensate parameter uncertainty and disturbance which varies with tyre-road conditions. The adaptation law (equations (19) and (20)) consists of a tracking error (i.e., $S(t)$) correction term. An adaptation law is rewritten in terms of Laplace transform as follows:

$$\hat{B}(s) = \frac{\eta_1 k_1}{s + \eta_1 k_1} B + \left(\frac{2k_1}{I_z v_x}\right)\frac{1}{s + \eta_1 k_1}\gamma S \tag{21}$$

$$\hat{C}_f(s) = \frac{\eta_2 k_2}{s + \eta_2 k_2} C_f + \left(\frac{2k_2 l_f}{I_z}\right)\frac{1}{s + \eta_2 k_2}\delta_f S \tag{22}$$

where the small s is a Laplace variable.

Theorem 1: *Considering vehicle yaw dynamics with designed sliding surface, the trajectory of the closed-loop control system can be driven on to the sliding surface $S(t) = 0$ with the proposed adaptive control law and adaptation update law, and finally converge to the pre-defined reference trajectory.*

Proof: Consider the following positive definite Lyapunov function:

$$V = \frac{1}{2}S^2 + \frac{1}{2k_1}\tilde{B}^2 + \frac{1}{2k_2}\tilde{C_f}^2. \tag{23}$$

The time derivative of equation (23) is as follows:

$$\begin{aligned}\dot{V} &= S\dot{S} + \frac{1}{k_1}\tilde{B}\dot{\hat{B}} + \frac{1}{k_2}\tilde{C}_f\dot{\hat{C}}_f = S(\dot{\gamma} - \dot{\gamma}_d) + \frac{1}{k_1}\tilde{B}\dot{\hat{B}} + \frac{1}{k_2}\tilde{C}_f\dot{\hat{C}}_f \\ &= S\left[\frac{2\gamma}{I_z v_x}\tilde{B} - \frac{2l_f\delta_f}{I_z}\tilde{C}_f - k_P S - k_S \cdot \mathrm{sgn(S)} + \frac{\bar{M}_d}{I_z}\right] + \frac{1}{k_1}\tilde{B}\dot{\hat{B}} \\ &\quad + \frac{1}{k_2}\tilde{C}_f\dot{\hat{C}}_f.\end{aligned} \tag{24}$$

With the adaptation laws, this can be rewritten as follows:

$$\begin{aligned}\dot{V} &= S\dot{S} + \frac{1}{k_1}\tilde{B}\dot{\hat{B}} + \frac{1}{k_2}\tilde{C}_f\dot{\hat{C}}_f = S(\dot{\gamma} - \dot{\gamma}_d) + \frac{1}{k_1}\tilde{B}\dot{\hat{B}} + \frac{1}{k_2}\tilde{C}_f\dot{\hat{C}}_f \\ &= S\left[\frac{2\gamma}{I_z v_x}\tilde{B} - \frac{2l_f\delta_f}{I_z}\tilde{C}_f - k_P S - k_S \cdot \mathrm{sgn(S)} + \frac{\bar{M}_d}{I_z}\right]\end{aligned}$$

$$
\begin{aligned}
&+\frac{1}{k_1}\tilde{B}\left(-\frac{2k_1}{I_z v_x}\gamma S-\eta_1 k_1\tilde{B}\right)\\
&+\frac{1}{k_2}\tilde{C}_f\left(-\frac{2l_f k_2}{I_z}\delta_f S-\eta_2 k_2\tilde{C}_f\right)\\
&=-k_P S^2-k_S|S|+S\cdot\left(\frac{\bar{M}_d}{I_z}\right)-\eta_1\tilde{B}^2-\eta_2\tilde{C}_f^2\\
&\leq -k_P S^2-k_S|S|+|S|\cdot\left|\frac{\bar{M}_d}{I_z}\right|-\eta_1\tilde{B}^2-\eta_2\tilde{C}_f^2\\
&\leq -k_P \mathrm{S}^2-(k_S-\Gamma)|\mathrm{S}|-\eta_1\tilde{B}^2-\eta_2\tilde{C}_f^2\ <0. \qquad (25)
\end{aligned}
$$

This shows that the tacking error $S(t)$ asymptotically converges to zero and the yaw stabilisation is also achieved.

Remark 3: The control parameters k_P and k_S in control law (equation (18)) play a important role in the control system. These parameters determine the convergence rate of the sliding surface. It is noted that a larger k_P will force the yaw rate to converge to the desired yaw rate trajectory with a high speed. However, in practice, a compromise between the response speed and control input should be made, since a too big k_P will require a very high control input, which is always bounded in reality. Therefore, the control parameter k_P can not be selected too large.

Figure 4 Description of: (a) signum function and (b) saturation function

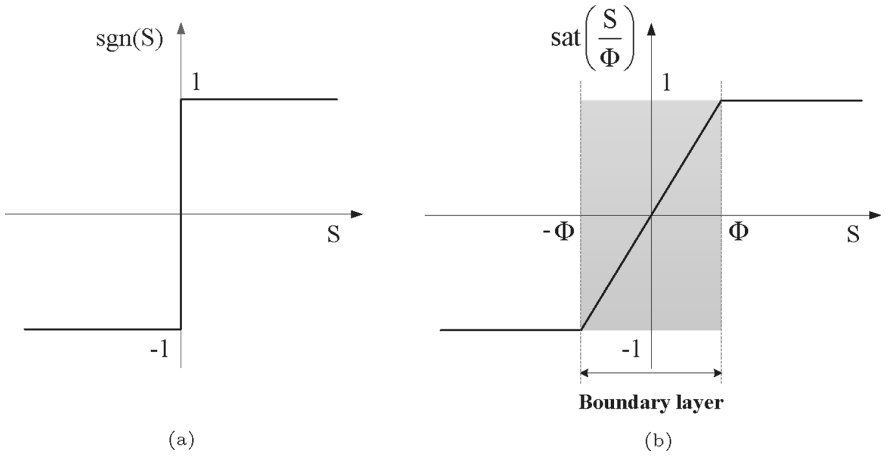

Remark 4: The control law (equation (18)) is discontinuous when crossing the sliding surface $S(t)=0$, which may lead to the undesirable chattering problem owing to the measurement noise and some actuator delay. This problem can be greatly alleviated by replacing a discontinuous switching function (see Figure 4) with a saturation function sat(S) with the boundary layer thickness Φ as the continuous approximation of a signum function

$$\text{sgn}(S) \approx \text{sat}\left(\frac{S}{\Phi}\right) = \begin{cases} \dfrac{S}{\Phi}, & \text{if } \left|\dfrac{S}{\Phi}\right| < 1 \\ \text{sgn}\left(\dfrac{S}{\Phi}\right), & \text{otherwise.} \end{cases} \tag{26}$$

Thus, this offers a continuous approximation to the discontinuous sliding mode control law inside the boundary layer and guarantees the motion within the neighbourhood of the sliding surface.

By applying the saturation function instead of the signum function, the chattering phenomenon can be decreased, but the tracking performance deteriorates. By adjusting the thickness of the boundary layer, the chattering phenomenon and the tracking error can be traded off. That is, if the thickness of the boundary layer is close to zero, then the controller acts like the sliding mode controller with a signum function, which shows more chattering and less tracking error. On the contrary, if the thickness of the boundary layer is large, then the chattering phenomenon disappears but the tracking performance is much deteriorated.

3.5 In-wheel-motor torque distribution

The control yaw moment M_z is distributed to two front in-wheel motors based on following equations (Fujimoto et al., 2005).

$$M_z = \frac{d}{2}(F_{fr}^x - F_{fl}^x)\cos\delta_f \tag{27}$$

$$T_{\text{cmd}} = T_{fl}^m + T_{fr}^m \tag{28}$$

where it is assumed that the vehicle is front wheel driving, the torque control commands to two front in-wheel motors are calculated as $T_{fl}^m = rF_{fl}^x$ and $T_{fr}^m = rF_{fr}^x$, respectively.

4 Experimental verification

The proposed adaptive sliding mode controller was implemented on the experimental IWM-EV shown in Figure 5(a). An experimental electric vehicle which was developed by the Hori/Fujimoto research team is equipped with direct-drive motors in each wheel. Figure 5(b) illustrates the driving motor installed in each wheel. The specification of an experimental electric vehicle used in field tests is presented in Table 1.

To demonstrate the performance and effectiveness of the proposed adaptive sliding mode controller, field tests were carried out with following driving conditions:

- constant vehicle speed, e.g., v_x = 35 km/h,
- step steering command, e.g., δ_{cmd} = 0.15 rad
- a proposed controller begins to work by enabling the manual control switch
- front-wheel driving mode
- dry asphalt.

Figure 5 Experimental in-wheel-motor-driven electric vehicle: (a) experimental IWM-EV and (b) in-wheel motor (see online version for colours)

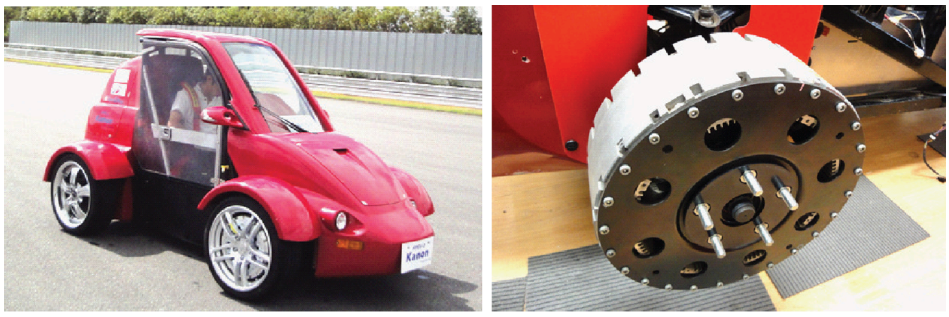

(a) (b)

Table 1 Specification of an experimental electric vehicle

Total weight	875 kg
Wheel base	1.715 m
Track width	1.3 m
Yaw moment of inertia	617 kg·m^2
Spin inertia for each wheel	1.26 kg·m^2
In-wheel motor	PMSM (outer rotor type)
Max. Power	20.0 kW (for one front motor)
Max. torque	500 Nm (for one front motor)
Max. speed	1113 rpm
Controller	AutoBox-DS1103
Steering system	Steer-by-wire
Suspension system	Double wishbone type
Battery	Lithium-ion

Figures 6 and 7 show the experimental results for the proposed adaptive sliding mode controller. A controller begins to work when the control switch (see the thick black line in Figure 6(c)) is turned on by a driver. A step steering input has been commanded by a driver at $t = 3.5$ s and the steering motor controller has worked for tracking the driver's steering command. Figure 6(a) shows the driving conditions including vehicle speed and lateral acceleration. The control law, which is generated from the proposed controller, is allocated to front left and right motors. Measured torques of front left and right in-wheel motors are illustrated in Figure 6(b). Figure 6(c) represents the results for yaw rate control. We can confirm that the proposed adaptive sliding mode controller stabilises the vehicle motion from the result of Figure 6(a). At $t = 17$ s, the controller began to work and an actual vehicle yaw rate tracks the desired yaw rate without a noticeable tracking error as shown in Figure 6(d). Even though the vehicle is in a critical driving situation (see the result of lateral acceleration in Figure 6(a)), the proposed adaptive sliding mode controller shows good tracking ability. Figure 6(e) and (f) show the results for parameter adaptation by equations (21) and (22). With the same driving conditions and somewhat narrowed boundary layer (i.e., $\Phi = 0.05$), experiments are performed for confirming the influences of the boundary layer. By comparing results of Figure 6 ($\Phi = 0.069$) and Figure 7 ($\Phi = 0.05$),

we can confirm that the chattering phenomenon can be decreased by adjusting the boundary layer. In addition, chattering reduction by using adjustable boundary layer is confirmed through results of Figure 8.

Figure 6 Experimental results of a step steering (i.e., $\delta_f = 0.15$ rad) test at $v_x = 35$ km/h on dry asphalt: (a) driving condition; (b) control motor torque; (c) yaw rate; (d) sliding surface: tracking error; (e) estimated parameter: $\hat{B}$ and (f) estimated parameter: $\hat{C}_f$ (see online version for colours)

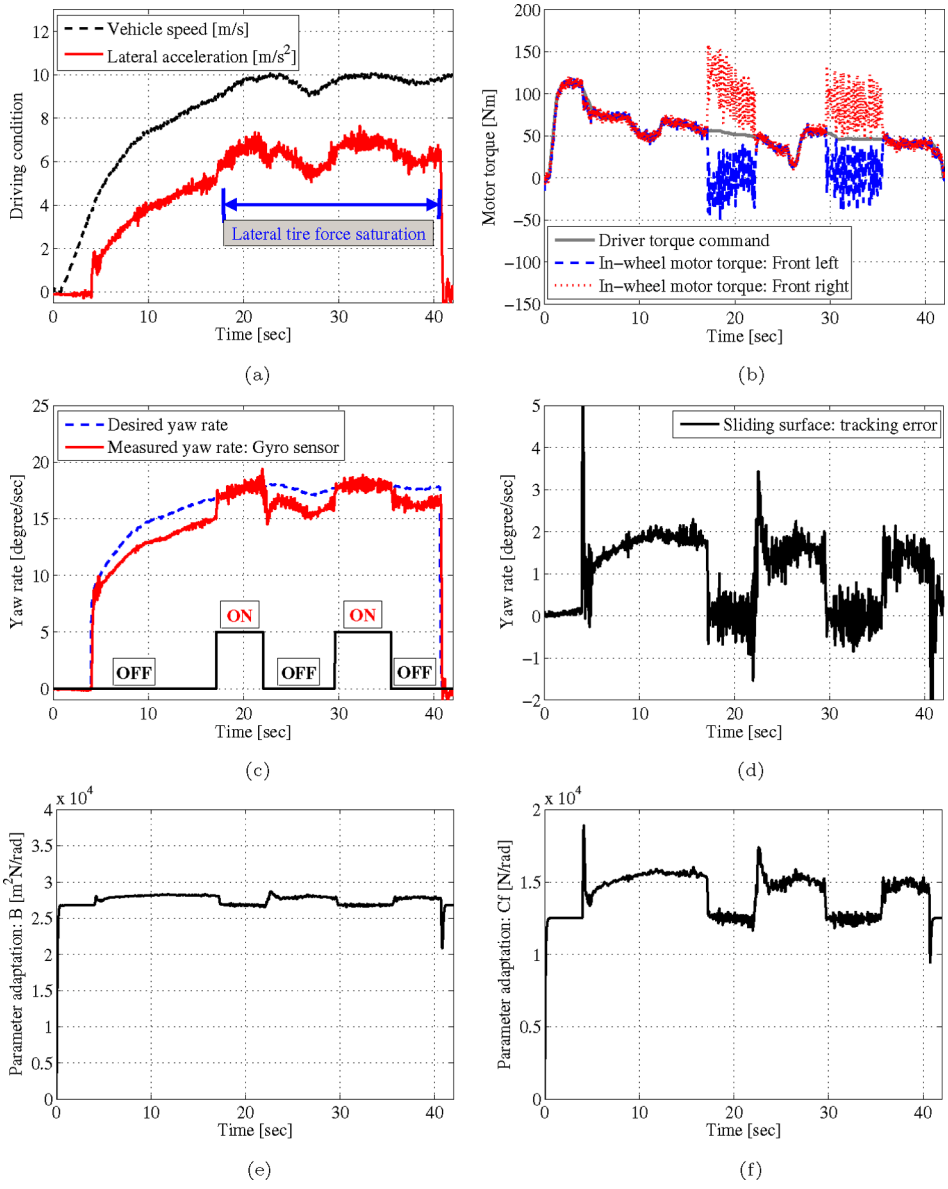

In short, the effectiveness of the proposed adaptive sliding mode controller is verified through experimental results of Figures 6 and 7. The sliding surface S(t), which indicates

a tracking error of the yaw rate, has converged to zero as shown in Figures 6(c) and 7(c). Through theoretical and experimental verification, it is confirmed that tracking performances and stability of the proposed adaptive sliding mode controller are achieved.

Figure 7 Experimental results of a step steering (i.e., $\delta_f = 0.15$ rad) test at $v_x = 35$ km/h on dry asphalt: (a) driving condition; (b) control motor torque; (c) yaw rate; (d) sliding surface: tracking error; (e) estimated parameter: $\hat{B}$ and (f) estimated parameter: $\hat{C}_f$ (see online version for colours)

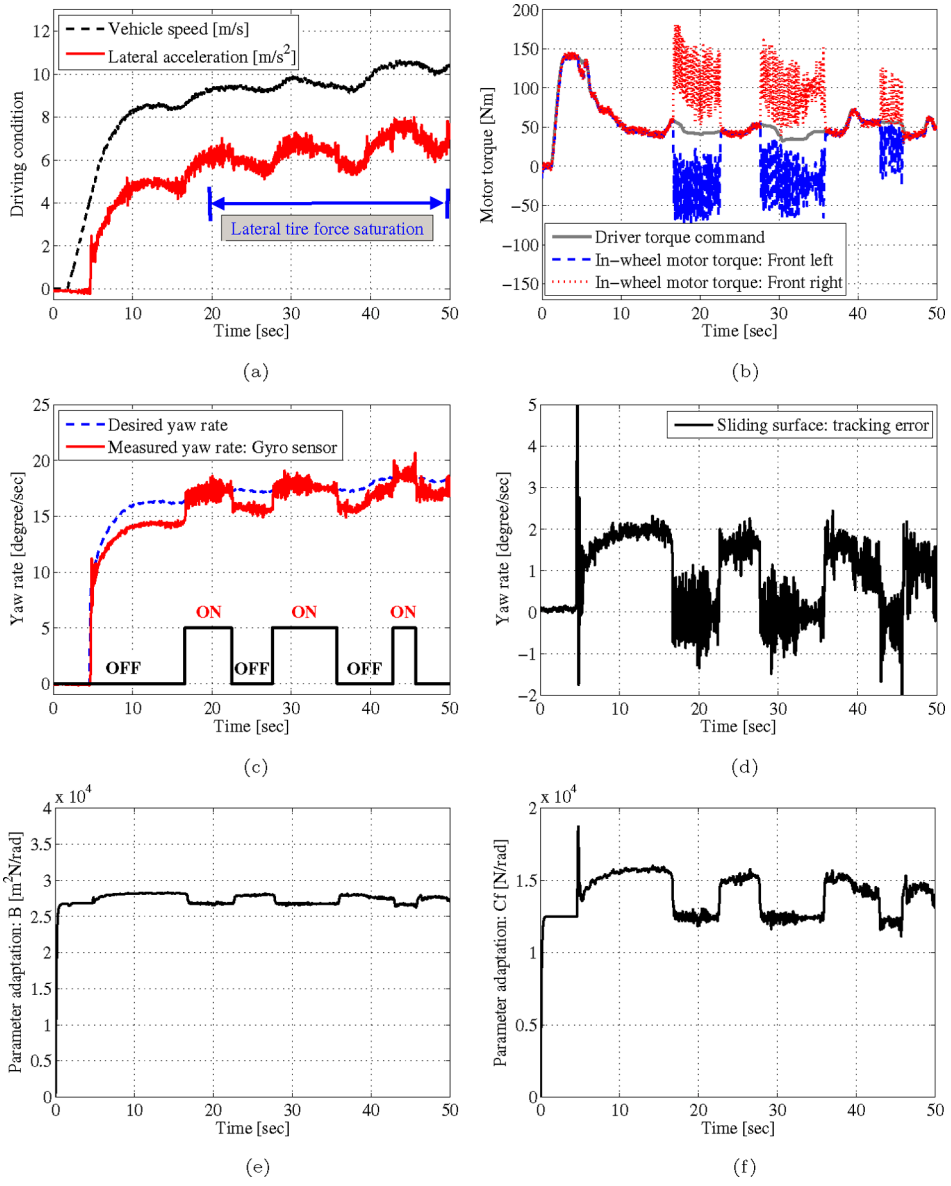

Figure 8 Effect of boundary layer on chattering reduction: (a) Sliding surface: tracking error; (b) sliding surface: tracking error (zoomed) and (c) sliding surface: tracking error (short time span) (see online version for colours)

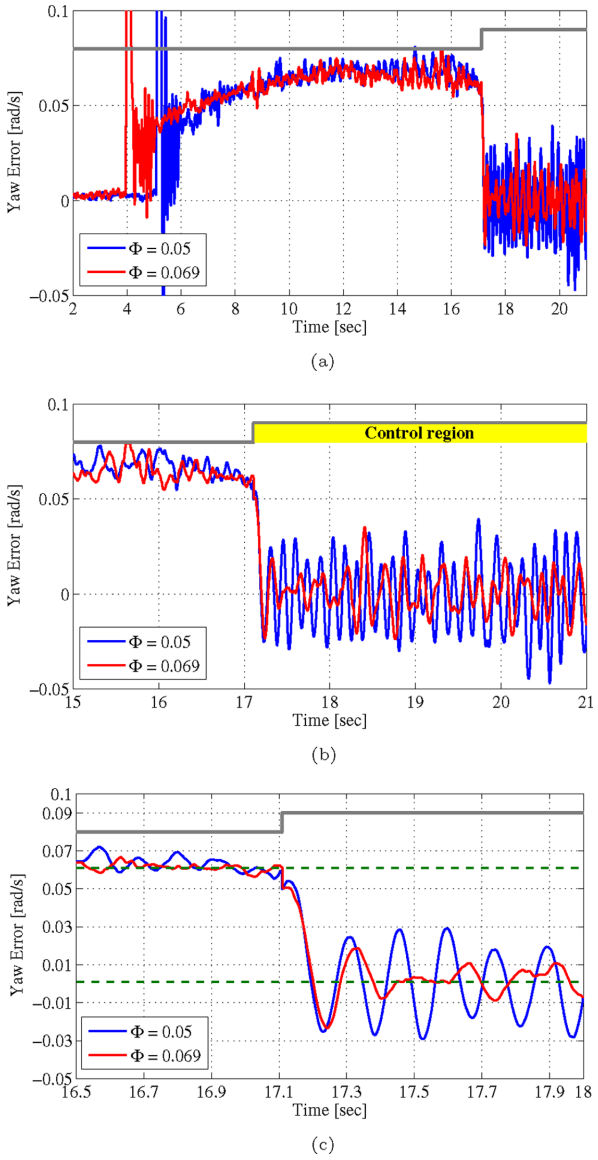

5 Conclusion and future works

This paper has presented an adaptive sliding mode control method for yaw stability enhancement of in-wheel-motor-driven electric vehicles. The proposed control structure is composed of a reference generator, a feedback controller (i.e., sliding mode controller), and parameter adaptation laws. The sliding mode control method, which is capable of guaranteeing robust stability in the presence of model uncertainties and disturbances, is

used to stabilise the vehicle yaw motion. Field tests using an experimental electric vehicle are carried out and its effectiveness is verified. In future works, optimal motor torque distribution methods will be presented and incorporated into the proposed adaptive sliding mode controller.

References

Canale, M., Fagiano, L., Ferrara, A. and Vecchio, C. (2008) 'Vehicle yaw control via second-order sliding mode control', *IEEE Trans. Ind. Electron.*, Vol. 55, No. 11, pp.3908–3916.

Fujimoto, H., Tsumasaka, A. and Noguchi, T. (2005) 'Direct yaw-moment control of electric vehicle based on cornering stiffness estimation', *Proc. of IEEE IECON*, November.

Gao, W. and Hung, J.C. (1993) 'Variable structure control of nonlinear systems: a new approach', *IEEE Trans. Ind. Electron.*, Vol. 40, No. 1, pp.45–55.

Cong, G., Mostefai, L., Denai, M. and Hori, Y. (2009) 'Direct yaw-moment control of an in-wheel-motored electric vehicle based on body slip angle fuzzy observer', *IEEE Trans. Ind. Electron.*, Vol. 56, No. 5, pp.1411–1419.

Hori, Y. (2004) 'Future vehicle driven by electricity and control-research on four-wheel-motored 'UOT electric March II'', *IEEE Trans. Ind. Electron.*, Vol. 51, No. 5, pp.654–962.

Kim, K., Hwang, S. and Kim, H. (2008) 'Vehicle stability enhancement of four-wheel-drive hybrid electric vehicle using rear motor control', *IEEE Trans. Veh. Technol.*, Vol. 57, No. 2, pp.727–735.

Kim, J., Park, C., Hwang, S., Hori, Y. and Kim, H. (2010) 'Control algorithm for an independent motor-drive vehicle', *IEEE Trans. Veh. Technol.*, Vol. 59, No. 7, pp.3213–3222.

Magallan, G.A., De Angelo, C. H. and Garcia, G.O. (2011) 'Maximization of the traction forces in a 2WD electric vehicle', *IEEE Trans. Veh. Technol.*, Vol. 60, No. 2, pp.369–380.

Mutoh, N. and Nakano, Y. (2012) 'Dynamics of front-and-rear-wheel-independent-drive-type electric vehicles at the time of failure', *IEEE Trans. Ind. Electron.*, Vol. 59, No. 3, pp.1488–1499.

Nam, K., Oh, S., Fujimoto, H. and Hori, Y. (2011) 'Vehicle state estimation for advanced vehicle motion control using novel lateral tire force sensors', *American Control Conf.*, Sanfrancisco, pp.4853–4858.

Nam, K., Fujimoto, H. and Hori, Y. (2012a) 'Lateral stability control of in-wheel-motor-driven electric vehicles based on sideslip angle estimation using lateral tire force sensors', *IEEE Trans. Veh. Technol.*, Vol. 61, No. 5, pp.1972–1985.

Nam, K., Oh, S., Fujimoto, H. and Hori, Y. (2012b) 'Robust yaw stability control for electric vehicles based on active front steering control through steer-by-wire (SbW) system', *International Journal of Automotive Technology*, Vol. 13, No. 5, pp.1169–1176.

Slotine, J.J.E. and Li, W. (1991) *Applied Nonlinear Control*, Prentice-Hall, Englewood Cliffs, NJ.

Tchamna, R. and Youn, I. (2013) 'Yaw rate and side-slip control considering vehicle longitudinal dynamics', *International Journal of Automotive Technology*, Vol. 14, No. 1, pp.53–60.

Wang, R. and Wang, J. (2011) 'Fault-tolerant control with active fault diagnosis for four-wheel independently-driven electric ground vehicles', *IEEE Trans. Veh. Technol.*, Vol. 60, No. 9, pp.4276–4287.

Yin, D., Oh, S. and Hori, Y. (2009) 'A novel traction control for EV based on maximum transmissible torque estimation', *IEEE Trans. Ind. Electron.*, Vol. 56, No. 6, pp.2086–2094.

Zhou, H. and Liu, Z. (2010) 'Vehicle yaw stability-control system design based on sliding mode and backstepping control approach', *IEEE Trans. Veh. Technol.*, Vol. 59, No. 7, pp.3674–3678.